Experimental campaign on thin RC columns prone to out-of-plane instability: numerical simulation using shell element models

Campaña experimental de columnas delgadas de concreto reforzado propensas a inestabilidad por fuera del plano: simulación numérica usando elemento tipo cáscara

Angelica Rosso[1*], Lisandro A. Jiménez-Roa[2], João P. Almeida[1] and Katrin Beyer[1]

[1]EESD, École Polytechnique Fédérale de Lausanne (EPFL), Lausanne, Switzerland
[2]Civil Engineering School, Universidad del Valle, Cali, Colombia

ABSTRACT

Construction of multi-storey reinforced concrete (RC) wall buildings in areas of moderate to high seismicity has become a common practice in several Latin-American countries such as Colombia, Peru, Ecuador and Mexico. The large material cost has led to the common practice of designing walls with only one layer of reinforcement and very low thickness. The earthquakes in Chile (2010) and New Zealand (2011) have shown that such design approach can induce out-of-plane failure of the walls under seismic action. In order to study the influence of different parameters on the out-of-plane response of thin members, an experimental campaign on RC columns was recently carried out at École Polytechnique Fédérale de Lausanne. These columns, axially loaded in cyclic tension-compression, represent the boundary element regions of RC walls, which correspond to the parts of the wall mainly involved in the instability mechanism.

This paper illustrates the application of a shell model with truss elements to simulate the response of the tested specimens. The accuracy of the numerical model is assessed by comparison against the experimental results. It is shown that good estimates of the critical tensile strain that leads to out-of-plane instability as well as the out-of-plane displacement in cycles prior to failure are obtained. The failure mode is adequately simulated and also local behaviour is consistently reproduced. Therefore, the application of similar models to assess the vulnerability of thin RC walls to out-of-plane instability appears to be a relatively simple and robust numerical tool for engineering practice.

Keywords: Out-of-plane Instability, Reinforced Concrete Boundary Elements, Large-scale Tests, Numerical Simulation.

RESUMEN

La construcción de edificaciones de muros de concreto reforzado (CR) de varios niveles en áreas de moderada a alta sismicidad, se ha convertido en una práctica frecuente en varios países Latinoamericanos como Colombia, Perú, Ecuador y México. Debido a los elevados costos en los materiales, se ha generado una práctica común de diseñar muros con una sola capa de reforzamiento y espesores muy bajos. Los terremotos ocurridos en Chile (2010) y Nueva Zelanda (2011) han demostrado que tal enfoque de diseño puede inducir una falla por fuera del plano del muro bajo la acción de cargas sísmicas. Con el fin de estudiar la influencia de diferentes parámetros en la respuesta por fuera del plano de miembros delgados, una campaña experimental sobre columnas de CR fue llevada a cabo recientemente en la École Polytechnique Fédérale de Lausanne. Estas columnas cargadas axialmente con ciclos de tensión-compresión, representan las regiones de elementos de borde de muros de CR, que corresponden a las partes del muro que están principalmente implicadas en el mecanismo de inestabilidad.

Éste artículo ilustra la aplicación de un modelo empleando elementos tipo cáscara y elementos tipo cercha para simular la respuesta de los especímenes ensayados. La precisión del modelo numérico se evalúa haciendo una comparación con los resultados experimentales. Se observa que se puede obtener una buena estimación de la carga crítica a tracción que genera la inestabilidad por fuera del plano, así como la estimación aproximada del desplazamiento máximo por fuera del plano alcanzado en los ciclos previos a la falla. El mecanismo de falla se simula adecuadamente, además se logra la reproducción consistente de resultados locales. Por lo tanto, la aplicación de modelos similares para evaluar la vulnerabilidad de muros delgados de CR en la inestabilidad por fuera del plano, aparenta ser una herramienta numérica relativamente simple y robusta para la práctica en ingeniería.

Palabras clave: inestabilidad por fuera del plano, elementos de borde de concreto reforzado, simulación numérica.

---

[*] Autor Correspondencia: angelica.rosso@epfl.ch

El presente artículo hace parte de las memorias del VIII Congreso Nacional de Ingeniería Sísmica organizado por la Universidad del Norte y la Asociación Colombiana de Ingeniería Sísmica. Área Metropolitana de Barranquilla, Mayo de 2017.

1 INTRODUCTION

Recent earthquakes in Chile (2010) and New Zealand (2011) have shown that, despite many years of extensive research and subsequent design code advancements, many reinforced concrete (RC) walls underperform during seismic events (Kam et al., 2011; Wallace et al., 2012). Some of the observed structural failures are not yet completely understood (NIST, 2014; Sritharan et al., 2014). In particular, lateral instability of several wall boundary regions had led to wall failures, which corresponds to a buckling type of failure that had previously been observed primarily in laboratory tests (Rosso et al., 2016).

Thin walls have shown to be particularly vulnerable to out-of-plane instability (Rosso et al., 2016). This issue is notably of interest considering that over the last few years, due to the high material costs, in several Latin American countries—such as Colombia, Peru, Ecuador and Mexico—many new residential buildings were constructed with thin walls and a light amount of reinforcing steel placed in a single layer. It should be underlined that in Colombia the wall thicknesses are as low as 8 cm, while in Chile and New Zealand the minimum wall thickness is nearly twice as large (15 cm). It is therefore to be feared that critical walls from these South American buildings may develop out-of-plane failures during a major earthquake if no retrofit interventions are carried out beforehand.

The first authors who studied the instability of RC walls were Goodsir and Paulay in 1985 (Goodsir, 1985; Paulay and Goodsir, 1985). The development of the out-of-plane mechanism can be summarized as follows (Paulay and Priestley, 1993; Chai and Elayer, 1999): at large in-plane curvature demands the boundary element develops large tensile strains that cause wide near-horizontal cracks and yielding of the longitudinal reinforcement in tension. Upon unloading, an elastic strain recovery takes place but due to the plastic tensile strains accumulated in the rebars the cracks remain open. Therefore, when reloading in compression and before crack closure, the compression force is resisted solely by the vertical reinforcement. This stage is typically accompanied by an incipient out-of-plane displacement, which occurs due to construction misalignments in the position of the two layers of reinforcement, eccentricity of the single layer of reinforcement, or eccentricity of the resultant vertical force. As compression increases, the longitudinal reinforcement may yield, leading to an abrupt reduction in out-of-plane stiffness and a consequent increase in the corresponding displacements. Depending on the magnitude of the tensile strain previously attained (i.e., before unloading), the cracks may close, re-establishing compressive force transfer through concrete and contributing to straighten up the wall, or they may remain open causing an abrupt increase of the out-of-plane displacements due to the reinforcement behaviour, possibly leading to wall buckling failure. Intermediate conditions, wherein cracks close at least partially, are also conceivable. Independently of the scenario that effectively takes place, the occurrence of out-of-plane displacements and second-order moments will affect the in-plane wall response and should therefore be taken into account. The existing models developed to describe the out-of-plane buckling of RC walls (Paulay and Priestley, 1993; Chai and Elayer, 1999) assimilate the boundary region—which represents the part of the wall mainly involved in the instability mechanism—to an equivalent column axially loaded in tension and compression. The parameter that governs the occurrence of out-of-plane deformations has long been identified as the magnitude of the maximum applied tensile strain prior to subsequent loading in compression (Paulay and Priestley, 1993). Past tests on RC columns loaded in tension and compression (Goodsir, 1985; Chai and Elayer, 1999; Acevedo et al., 2010; Creagh et al., 2010; Chrysanidis and Tegos, 2012; Hilson et al., 2014; Menegon et al., 2015; Taleb et al., 2016; Welt et al., 2016) have confirmed this assumption. In these experimental campaigns, however, the influence of various parameters such as wall thickness, presence of a single layer of reinforcement and its eccentricity with respect to the centreline of the section, or the reinforcement ratio, was only marginally addressed.

In the following, an experimental campaign on 12 equivalent RC thin columns, representative of wall boundary elements with a single layer of vertical reinforcement, carried out at École Polytechnique Fédérale de Lausanne (EPFL) within a collaborative project with three Colombian universities (University of Valle, E.I.A. University and the University of Medellin) is briefly presented. Namely, a description of the geometric and material properties of the specimens, of the test setup, and of the loading protocols is shown. Then, a shell model with truss elements is used to assess the behaviour of the test units. The main features of the numerical model are presented, followed by a comparison with the experiments. It is shown that the finite element model provides a good estimate of the maximum tensile strain causing the out-of-plane failure, an accurate description of the development of instability, and a satisfactory agreement when comparing also local level measures.

2 DESCRIPTION OF THE EXPERIMENTAL CAMPAIGN

The tested columns are representative of full-scale equivalent boundary elements of thin walls. The height of the test units is 2.4 m (see Figure 1a), representative of the typical Colombian interstorey height. This choice is further motivated by recent experimental results from two thin RC walls (Rosso et al., 2016), which suggested that almost the entire height of the first storey is involved in the out-of-plane mechanism. The cross-section of all the specimens was 300 mm long (see also Figure 1a), and the longitudinal reinforcement was placed in a single layer, eccentrically with respect to the centreline of the section. The horizontal reinforcement consisted of 16 bars of diameter 6 mm, spaced of 150 mm. The column foundation and head were RC blocks designed as stiff rigid members. The geometric characteristics and the material properties of the concrete and reinforcement of each thin column (herein denoted with the acronym ‘TC’) are summarised in Table 1, whilst the results of the full experimental campaign can be found in Rosso, Jimenez, et al., (2017).

The tests were performed in deformation control. The vertical displacement was averaged from the measurements provided by four vertical LVDTs gaging the elongation between the upper face of the foundation block and the lower face of the top column block (three out of four LVDTs can be seen in Figure 1b). The three-dimensional displacement fields of the two shorter column sides (i.e., North and South faces, see Figure 1a) were recorded using an optical triangulation measurement system (NDI, 2009) through a grid of more than 180 infrared light emitting diodes (LEDs) glued to the surfaces (see Figure 1b-c). The LEDs were placed on the column at a regular spacing, as well as on the top and foundation blocks. The loading protocol consisted of the application of cyclic axial displacements. The peak displacements in compression were kept the same, corresponding to an average compressive strength of $0.3{\cdot}f_c$ assuming a linear elastic response. The peak displacements in tension were increased every other cycle. The following positive peak displacements were applied: 1.5 mm → 3 mm → 6 mm, and subsequently they were incremented by 3 mm.

All the specimens developed large out-of-plane deformations during loading (except specimen TC07, due to poor detailing and lower-than-requested steel ductility properties) and the tests were stopped when out-of-plane failure was attained (e.g., Figure 1c). The latter meant that concrete crushing took place in the compression side of the out-of-plane plastic hinges that formed, causing an irrecoverable increase on lateral displacement with further increase of the compressive load.

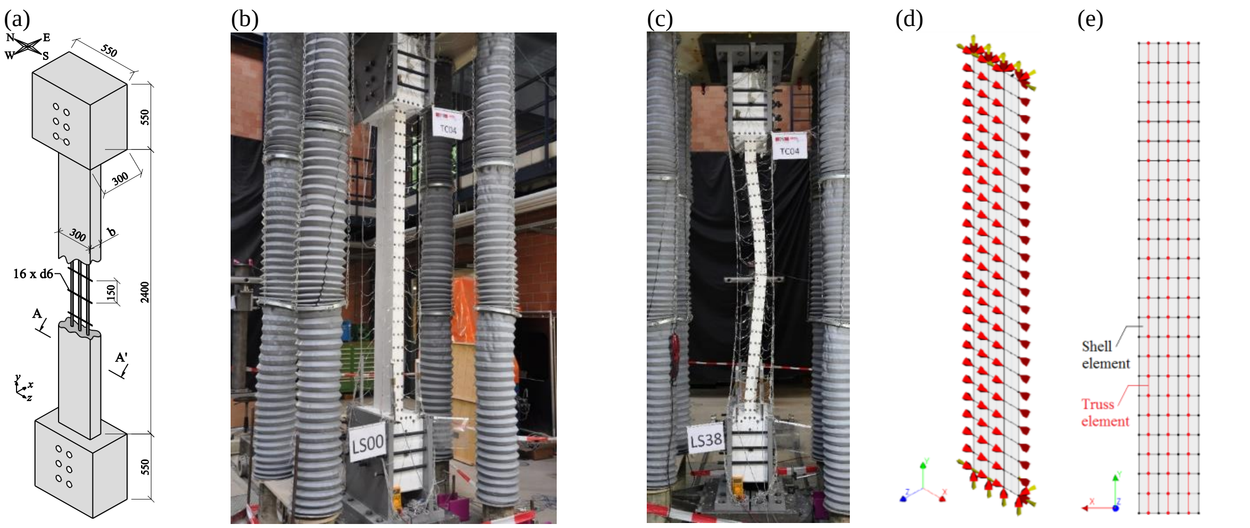

Figure 1: (a) Geometric characteristic of the boundary elements tested. (b) Test setup of the experimental campaign. (c) Specimen TC04 at attainment of out-of-plane failure. (d)-(e) DIANA model: detail of boundary conditions and discretisation.

Table 1: Description of the specimens tested in the experimental campaign.

Specimen	l mm	h mm	b mm	ρ %	d_b mm	No. bars -	e mm	f_c MPa	$f_{s,y}$ MPa	$f_{s,u}$ MPa
TC01	300	2400	80	0.35	6	3	8	23.7	475	625
TC02	300	2400	80	2.51	16	3	8	23.7	526	617
TC03	300	2400	100	0.85	6	9	8	25.7	475	625
TC04	300	2400	100	0.28	6	3	8	32.3	475	625
TC05	300	2400	100	0.79	10	3	8	25.7	545	582
TC06	300	2400	100	3.80	22	3	8	32.3	566	663
TC07	300	2400	100	2.09	10	8	8	25.7	545	582
TC08	300	2400	100	0.28	6	3	24	23.7	475	625
TC09	300	2400	100	2.01	16	3	24	32.3	526	617
TC10	300	2400	100	2.01	16	3	8	32.9	526	617
TC11	300	2400	100	2.01	16	3	8	32.9	526	617
TC12	300	2400	100	2.01	16	3	8	33.6	526	617

Legend l: length. h: height. b: thickness. ρ: longitudinal reinforcement ratio. d_b: rebar diameter. No. bars: number of rebars. e: eccentricity of the longitudinal reinforcement with respect to the centreline of the section. f_c: concrete compressive strength. f_y: rebar steel yield strength. f_u: rebar steel ultimate strength.

3 DESCRIPTION OF THE NUMERICAL MODEL

The columns, which represent the boundary element of a wall, were simulated with a shell element model. The 3D finite element model presented in this paper was created in the software DIANA (TNO 2016) using curved shell elements that allow capturing buckling and post-buckling response phases. A four-node quadrilateral isoparametric curved shell element, named *Q20SH*, is used. A grid of 11 × 4 (thickness × element plane) Gauss integration points is used. The reinforcement is modelled with embedded truss elements with two integration points, and each rebar is modelled through several truss elements. This choice is motivated by the nature of the out-of-plane instability phenomenon: when the column is subjected to axial loading, the vertical force is approximately constant while the bending moment varies along the height (particularly when second order effects become relevant). In the specific phase where the column is subjected to tensile loads, such variable internal forces along the height are equilibrated solely by the rebar when the cracks are fully open and the concrete does not contribute, which implies that the reinforcement is required to develop a resisting bending moment. For this reason, hence, it is necessary to discretize the rebar into several trusses (e.g., four in this specific work) and not only in one, which is the commonly used procedure when discretizing RC sections with fibres. The compressive behaviour of the concrete is modelled using an uniaxial Hognestad parabolic curve (Vecchio and Collins, 1993), while the tensile behaviour is represented as a linear tension softening. The ‘Total Strain Crack Model’ and the ‘Rotating Crack Model’ available in DIANA (TNO 2016) are employed. The steel behaviour follows the Monti-Nuti cyclic stress-strain law (Monti and Nuti, 1992). The boundary conditions set for the model (Figure 1d) consist of a total restriction of the six degrees of freedom at the base of the column (translations and rotations), while at the top only vertical translations are allowed. Additionally, all the nodal displacements along the *x* axis were also restrained in order to allow deformations only in the out-of-plane direction (see Figure 1d).

The numerical model was used to simulate the behaviour of the 12 specimens described in Section 2. The columns were discretised using 24 elements along the height and 3 along the width, in order to obtain a squared mesh (Figure 1e). The increments used to apply the imposed top displacements were 0.1 and 0.05 mm when loading and unloading respectively. To shorten the time of each analysis and reduce the risk of convergence problems, the numerical model is subjected to a single cycle of loading which first tensions the column and then compresses it.

4 COMPARISON BETWEEN EXPERIMENTAL AND NUMERICAL RESULTS

4.1 *Global behaviour*

Figure 2 shows the results of three specimens: TC01, TC02 and TC04. The latter were chosen as they are illustrative of several key findings that are worth to be highlighted. The experimental axial force-displacement curves (blue lines) are overlapped with the two obtained with numerical model, corresponding to the application of: (i) the largest tensile displacement for which an out-of-plane deformation recovery still takes place upon unloading and reloading in compression (red continuous lines); (ii) the smallest tensile displacement for which an out-of-plane failure is attained upon unloading and reloading in compression (red dashed lines). It can be observed that an accurate estimate of the critical tensile displacement causing failure is obtained for specimen TC01 (Figure 2a), while slightly non-conservative estimates are obtained for specimens TC02 and TC04.

(a) (b) (c)

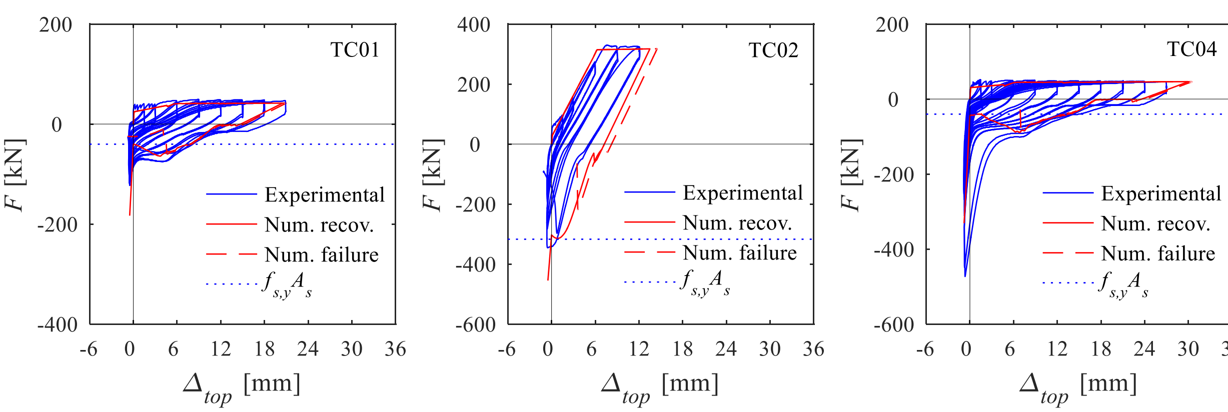

Figure 2: Comparison of experimental and numerical force-displacement (F-Δ_{top}) curves of specimens: (a) TC01, (b) TC02 and (c) TC04. Note that A_s is the total area of longitudinal reinforcement.

The experimental curves display a stable hysteretic behaviour with fair dissipation of energy and plastic deformation in tension. All the three test units attained out-of-plane failure, at which point a drop in the axial force takes place, which is clearly identifiable for instance in Figure 2b. In the branches where reloading in compression takes place, at low values of compressive force a plateau following a loss in stiffness can be observed. This plateau coincides with the development of out-of-plane deformations, showing that the onset of lateral displacements occurs at force values much lower than the yielding force ones (dotted lines in Figure 2). Such plateau can be relatively pronounced, such as in Figure 2a and Figure 2c, or almost undiscernible as in Figure 2b. This behaviour can be identified both in the numerical and experimental results. Moreover, it can be observed that the numerical model provides a good estimate of the maximum axial force, as well as of the stiffness of the specimens. However, a few differences can also be pointed out. Firstly, after having reached the maximum tensile displacement, the numerical model is not able to simulate the small drop that can be observed in the experimental response, which is an expected feature since the latter is related to the fact that, after each load stage, the tests were stopped for a time period and such break caused: (i) a small reduction in the testing machine pump pressure, and (ii) stress relaxation in the rebars and concrete. Secondly, at zero vertical displacement after unloading, in the numerical model the cracks close fully along the column, causing a sudden increase in the stiffness slope. The equivalent stiffness increase due to crack closure is less evident in the experimental curves because a more progressive phenomenon—affected by the roughness of the crack and small offsets along the crack—takes places.

Figure 3 illustrates the out-of-plane displacement at the height where it was maximum *vs* the vertical displacement imposed to the column. A first observation from experiments is that the columns slightly displaced out-of-plane when subjected to a tensile displacement, while a similar feature did not happen in the numerical model. Then, upon reduction of the applied vertical displacement, such lateral deformations reduced to zero and only after attaining a compressive force—as described above—did the out-of-plane displacements start to increase again. It is noted that these lateral deformations, both in the experiments and in the numerical simulation, started occurring at similar values of applied vertical displacement. The maximum value of out-of-plane displacement attained and recovered is in general larger in the numerical models.

Figure 4a shows a comparison of the out-of-plane profiles at maximum lateral deformation attained and subsequently recovered. With respect to the height at which the maximum out-of-plane displacement was attained, in the experimental campaign it varied significantly among the different specimens (within the entire campaign between 800 and 1400 mm), while in the numerical simulations the maximum occurred always almost at midheight due to the symmetry of the model. A key difference can be identified in the out-of-plane shape profiles: the experimental profiles are characterized by approximately piecewise-linear regions, while the numerical ones are essentially smooth. This can be explained by the distributed cracking that is simulated by the numerical model along the column height, which significantly differs from the concentrated rotational demands occurring experimentally at some discrete plastic hinges. This feature also manifests in distinct curvature profiles between the experimental and the numerical results (Rosso, et al. 2017). However, it can be said that overall the out-of-plane profile is captured satisfactorily by the shell element model, although the latter always overestimates it.

4.2 *Local behaviour*

The rows of LEDs glued along the column height allowed to compute discrete local strains within the thickness. Each of the 25 rows was formed by three LEDs—placed along the thickness close to the edges and at the centreline—and they were spaced vertically of 100 mm. The three strain measures obtained per pair of rows were interpolated and extrapolated linearly in order to obtain a continuous strain profile along the thickness, therefore providing estimates at the edges of the column thickness and at the location of the longitudinal reinforcement. These experimentally derived local strain measures (ε_{loc}) are compared with the numerical results in the following for specimen TC02.

The local strains calculated at the height where a plastic hinge formed (10 mm below the rigid head of the column) *vs* the out-of-plane displacements at the height where it was maximum are plotted in Figure 4b and c. The experimental strains (Figure 4b) refer to the edge along the thickness where the crack first closed, i.e., at the concave edge (intrados) of the out-of-plane deformed profile. The numerical strains (Figure 4c) were read from the finite element located at the same hinge height, on the concave edge of the out-of-plane deformed profile and at the outermost integration point.

First off, it is observed that when unloading starts the experimental strains are much larger than the global tensile strain imposed to the specimens (i.e., 0.5% at the last tensile displacement before failure). This strong localization effect in tension is not captured by the numerical model, in which the local and global vertical strains closely match. Secondly, a comparison of the two figures puts into evidence that a critical value of the compressive strain equal to 0.2% is only exceeded, both in the experiments and in the numerical model, when out-of-plane failure occurs. This value is commonly taken as representative of the attainment of the concrete compression strength, and therefore it appears that the onset of concrete crushing triggers unrecoverable out-of-plane deformations and consequent failure (Rosso, Jimenez, et al., 2017).

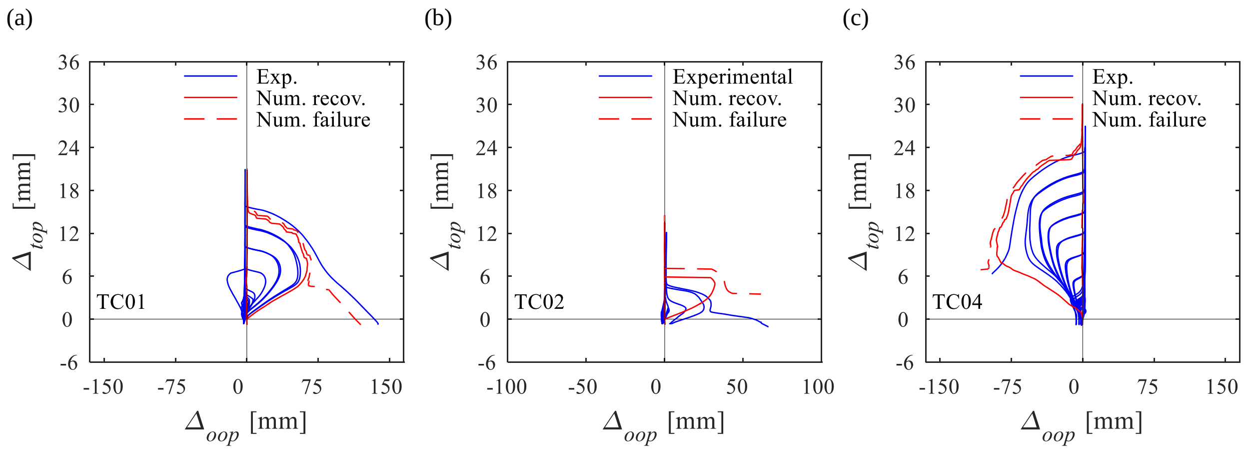

Figure 3: Out-of-plane displacement at the height where it was maximum (Δ_{oop}) *vs* vertical displacement imposed at the top of the column (Δ_{top}) for specimens: (a) TC01, (b) TC02, and (c) TC04.

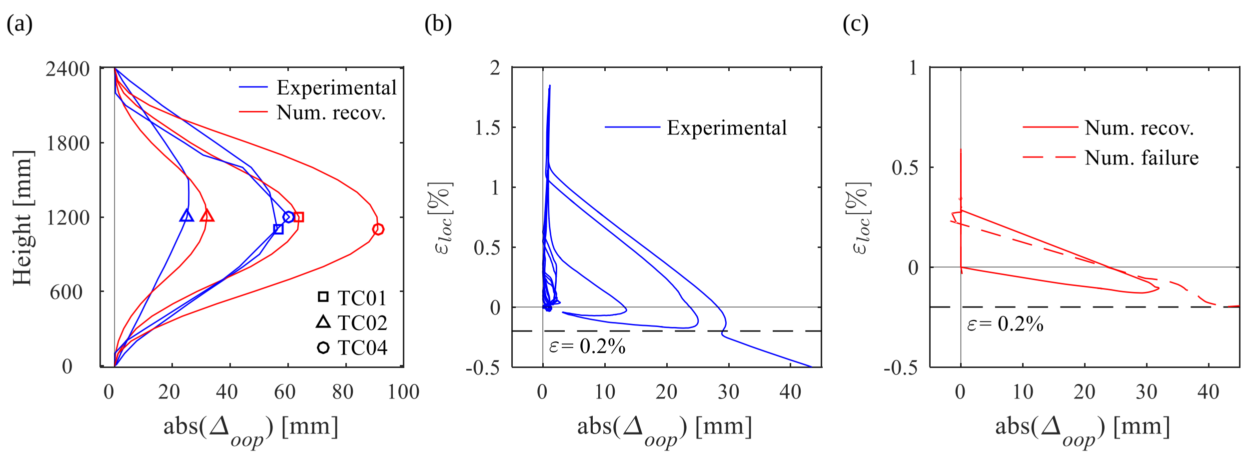

Figure 4: (a) Out-of-plane profile along the height at maximum lateral displacement attained (and subsequently recovered). (b)-(c) Out-of-plane displacement at the height where it was maximum *vs* local strain (ε_{loc}) on the edge along the thickness where the crack first closed, in a hinge at the top of specimen TC02: experimental and numerical results respectively.

Figure 5a shows the evolution of the axial strains at the rebar position (i.e., at an eccentricity of 8 mm from the centreline, as obtained from the interpolation of the measured strains) at the height of the previously mentioned plastic hinge *vs* the out-of-plane displacement at the height where it was maximum. It is recalled that the value of the rebar strain does not correspond to the actual steel strain in the crack, but to an interpolated value as described above. The figure indicates that, before the development of out-of-plane deformations, a sort of elastic strain recovery takes place. After this recovery, the strains remain almost constant whilst the out-of-plane displacements increases. It is interesting to compare the previous figure with Figure 4b. It can be noted that while the axial strains remain almost constant at the rebar position during the increase of out-of-plane deformations, the concrete strains at the extremities change from tensile to compressive values, indicating crack closure. This observation (which was observed in the remaining hinges and specimens) suggests that the mechanism of out-of-plane instability is different in members with one and two layers of longitudinal reinforcement. In fact, in a two-layer column—because of irregularities in the placement of the rebars and/or of variability in the position of the compression force—the layer of reinforcement closest to the compression resultant yields in compression (see green line in Figure 5c). Only when the stiffness of this layer reduces significantly due to Bauschinger effect and plasticization in compression will large curvatures and correspondingly large out-of-plane displacements develop. The crack will eventually close on the edge adjacent to the first rebar yielding in compression, since the second bar has not yet yielded and hence retains a relatively large stiffness (Paulay and Priestley, 1993). The development of this mechanism requires relatively large compressive forces in order to yield the first layer of reinforcement in compression, and thus one can expect onset of out-of-plane deformations for large compressive forces. On the other hand, as previously shown, in the case of a single-layer member, as soon as the member undergoes compressive forces the reinforcement in the crack acts like a hinge around which the column regions above and below the crack rotate (see Figure 5c) and therefore the column can develop large localized curvatures at small values of compressive forces (Rosso, Jimenez, et al., 2017).

In Figure 5b the strain in each of the four trusses that model each rebar (recall discussion in Section 3) is plotted, together with their average, *vs* the out-of-plane displacement for the model in which the lateral deformation was recovered. As mentioned before, the local strains are smaller than the experimental ones (Figure 5a), but a similar hinge-like behaviour of the reinforcement can be observed.

4.3 *Validation of the shell element model against experimental results*

The critical values of the tensile displacements causing out-of-plane failure, as derived from the shell element models, are compared with the experimental ones in Figure 6a using the ratio $\Delta_{top,cr,NUM}/\Delta_{top,cr,EXP}$, for the entire set of specimens in the experimental campaign. It is apparent that in general the numerical model is in quite good agreement with the experimental results (mean of 0.998 and coefficient of variation of 13.6%).

Figure 6b and c show the variation of the critical displacement with the reinforcement content (for the same thickness and eccentricity) and the thickness (for the same eccentricity) respectively. The numerical model is able to correctly reproduce the experimentally observed trends, which show that: (i) when the reinforcement content is increased, the vulnerability to out-of-plane instability also grows (Figure 6b), (ii) when the thickness is increased, the boundary element is less prone to out-of-plane failure (Figure 6c). Qualitatively, the trends obtained are also consistent with the phenomenological model by Paulay & Priestley (1993), assuming a plastic hinge length equal to half the total column height (Paulay and Priestley assume a pin-pin model, while in the present case the boundary conditions are fix-fix).

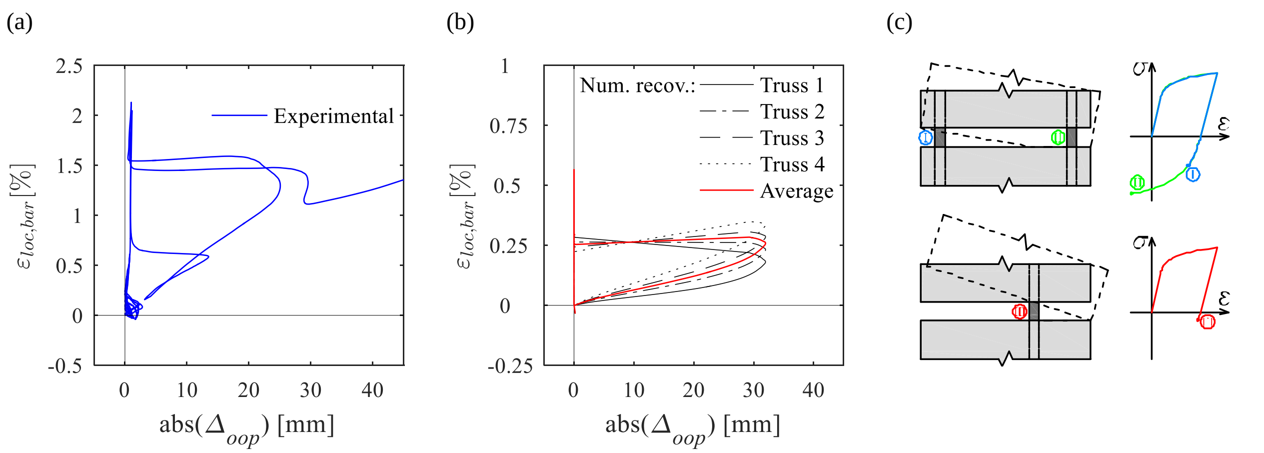

Figure 5: (a)-(b) Out-of-plane displacement at the height where it was maximum *vs* local strain at the rebar position ($\varepsilon_{loc,bar}$) in a hinge at the top of specimen TC02: experimental and numerical results respectively. (c) Description of the onset of out-of-plane instability for columns with one or two layers of reinforcement.

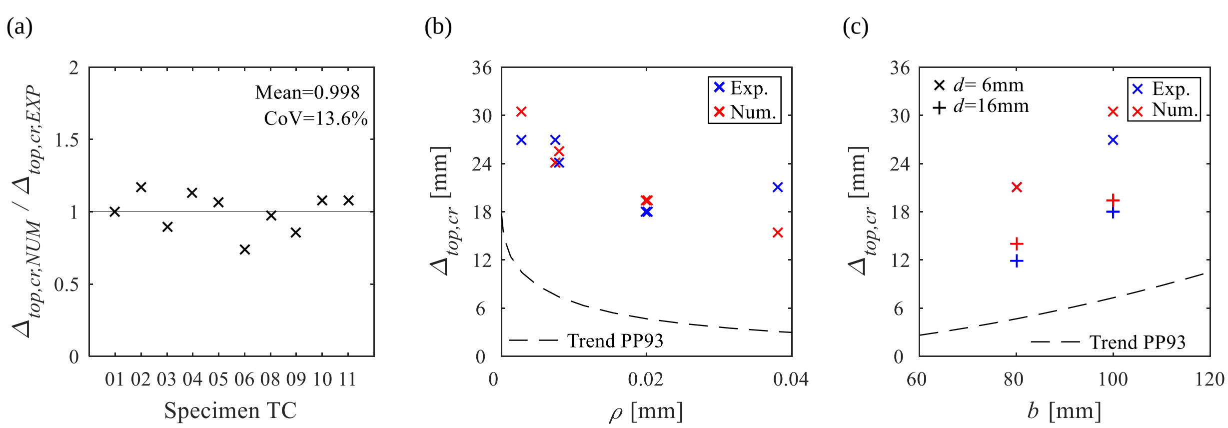

Figure 6: (a) Critical tensile displacement for the specimens in the experimental campaign: comparison between the numerical predictions and the experimental results. (b)-(c) Variations of the critical tensile displacement ($\Delta_{top,cr}$) with the reinforcement content (ρ) and the thickness (b) respectively.

CONCLUSIONS

In the present study a shell element model with truss elements was used to simulate the response of 12 thin reinforced concrete columns—representative of boundary regions of thin walls—recently tested under cyclic tensile-compressive loading with the purpose of studying the out-of-plane instability phenomenon. The accuracy of the numerical model was assessed by comparison against the experimental results, both at the global (axial and out-of-plane displacements) and the local (strains) level. It was shown that the failure mode is adequately simulated and that a reasonable estimate of the critical tensile strain triggering out-of-plane failure can be obtained. The out-of-plane behaviour of the specimens is satisfactorily reproduced, and local measurements are also acceptably simulated. Finally, it is shown that the shell element model is able to adequately reproduce the influence of key parameters on the out-of-plane response and failure. Therefore, the application of the described finite element model seems to be a reliable and relatively simple numerical tool to assess the vulnerability of thin RC walls to out-of-plane instability.

ACKNOWLEDGMENT

The testing of the specimens was financed through an *EPFL Seed Money* grant through the *EPFL Cooperation & Development Center*, which was awarded to the *EESD group* (PI) and the *University of Valle*, the *E.I.A. University* and the *University of Medellin*, in Colombia (Co-PIs). The first author is supported by the *Swiss National Science Foundation* grant 200021_132315 'Seismic design and assessment of reinforced concrete core walls - Phase II'. All contributions are gratefully acknowledged.

REFERENCES

Acevedo, C.E., A. Creagh, J.P. Moehle, et al. (2010). Seismic vulnerability of non-special boundary element of shear wall under axial force reversals. Report, Florida International University and University of California, Berkley, U.S.

Chai, Y.H., and D.T. Elayer. (1999). Lateral stability of reinforced concrete columns under axial reversed cyclic tension and compression. *ACI Structural Journal 96*, 1–10.

Chrysanidis, T.A., and I.A. Tegos. (2012). The influence of tension strain of wall ends to their resistance against lateral instability for low-reinforced concrete walls. *In* 15th World Conference on Earthquake Engineering, Lisboa, Portugal.

Creagh, A., C. Acevedo, J.P. Moehle, et al. (2010). Seismic performance of concrete special boundary element. Report, University of Texas at Austin and University of California Berkley, U.S.

DIANA TNO. (2016). Finite Element Analysis User's Manual - Release 10.1.

Goodsir, W.J. (1985). The design of coupled frame-wall structures for seismic actions. PhD Thesis, University of Canterbury, Christchurch, New Zealand.

Hilson, C.W., C.L. Segura, and J.W. Wallace. (2014). Experimental Study of Longitudinal Reinforcement Buckling in Reinforced Concrete Structural Wall Boundary Elements. *In* Tenth U.S. National Conference on Earthquake Engineering, Anchorage, Alaska.

Kam, W.Y., S. Pampanin, and K. Elwood. (2011). Seismic performance of reinforced concrete buildings in the 22 February Christchurch (Lyttleton) earthquake. *Bulletin of the New Zealand National Society for Earthquake Engineering 44*, 239–278.

Menegon, S.. J., J.. L. Wilson, E.. F. Gad, et al. (2015). Out-of-plane buckling of limited ductile reinforced concrete walls under cyclic loads. *In* 2015 NZSEE Conference, Rotorua, New Zealand.

Monti, G., and C. Nuti. (1992). Nonlinear Cyclic Behavior of Reinforcing Bars Including Buckling. *Journal of Structural Engineering 118*, 3268–3284.

NDI. (2009). Optotrak Certus HD, Northern Digital Inc. Available at: http://www.ndigital.com/industrial/certushd.php.

NIST. (2014). Recommendations for Seismic Design of Reinforced Concrete Wall Buildings Based on Studies of the 2010 Maule, Chile Earthquake. Report, National Institute of Standards and Technology, U.S. Department of Commerce.

Paulay, T., and W.J. Goodsir. (1985). The ductility of structural walls. *Bulletin of the New Zealand National Society for Earthquake Engineering 18*, 250–269.

Paulay, T., and M.J.N. Priestley. (1993). Stability of ductile structural walls. *ACI Structural Journal 90*, 385–392.

Rosso, A., J.P. Almeida, and K. Beyer. (2017). Numerical simulation with fibre beam-column models of thin RC columns under cyclic tensile-compressive loading. *In* 16th World Conference on Earthquake Engineering, Santiago, Chile.

Rosso, A., J.P. Almeida, and K. Beyer. (2016). Stability of thin reinforced concrete walls under cyclic loads: state-of-the-art and new experimental findings. *Bulletin of Earthquake Engineering 14*.

Rosso, A., L. Jimenez, J.P. Almeida, et al. (2017). Cyclic tensile-compressive testing of thin reinforced concrete boundary elements with a single layer of reinforcement prone to out-of-plane instability. *To be submitted to Bulletin of Earthquake Engineering*.

Sritharan, S., K. Beyer, R.S. Henry, et al. (2014). Understanding poor seismic performance of concrete walls and design implications. *Earthquake Spectra 30*, 307–334.

Taleb, R., M. Tani, S. Kono, et al. (2016). Performance of Confined Boundary Regions of RC Walls under Cyclic Reversal Loadings. *Journal of Advanced Concrete Technology 14*, 108–124.

Vecchio, F.J., and M.P. Collins. (1993). Compression response of cracked reinforced concrete. *Journal of Structural Engineering 119*, 3590–3610.

Wallace, J.W., L.M. Massone, P. Bonelli, et al. (2012). Damage and implications for seismic design of RC structural wall buildings. *Earthquake Spectra 28*, S281–S299.

Welt, T.S., L.M. Massone, J.M. LaFave, et al. (2016). Confinement Behavior of Rectangular Reinforced Concrete Prisms Simulating Wall Boundary Elements. *ASCE Journal of Structural Division 318*.